

N 7 3 - 1 6 6 7 4

**NASA TECHNICAL  
MEMORANDUM**

NASA TM X- 68187

NASA TM X- 68187

**CASE  
FILE  
COPY**

**THE REACTION  $pd \rightarrow t\pi$  AT 470 and 590 MeV**

by W. Dollhopf, C. Lunke, C. F. Perdrisat, W. K. Roberts,  
P. Kitching, W. C. Olsen, and J. R. Priest  
Lewis Research Center  
Cleveland, Ohio

**TECHNICAL PAPER proposed for presentation at  
1973 Annual Meeting of the American Physical Society  
New York, New York, January 29 - February 1, 1973**

# THE REACTION $pd \rightarrow t\pi^+$ AT 470 AND 590 MeV\*

by W. Dollhopf, <sup>†</sup> C. Lunke, <sup>‡</sup> C. F. Perdrisat, <sup>†</sup> W. K. Roberts,  
P. Kitching, <sup>\*\*</sup> W. C. Olsen, <sup>\*\*</sup> and J. R. Priest<sup>†\*</sup>

## Abstract

The preliminary results from a study of the  $d(p, \pi^+)t$  reaction are reported. The differential cross section for this reaction was measured for a number of center of mass angles from  $37^\circ$  to  $160^\circ$  at incident proton energies of 470 and 590 MeV. The cross sections measured at 590 MeV agree with predictions made considering a two-nucleon process. The 470 MeV data shows a peak in the backward direction which is not predicted by this mechanism.

E-7325

## Introduction

Pion production on nuclei in which the final state consists of a bound nucleus and a pion can be described in terms of one- and two-nucleon processes. A one-nucleon process occurs when the incident nucleon emits a pion before the nucleon is captured by the target nucleus. A two-nucleon process occurs when the incident nucleon interacts with a nucleon within the target nucleus causing a pion to be emitted with the incident nucleon being captured by the target nucleus. However, for energies around 600 MeV and above, the two-nucleon process should dominate. This is due to the high momentum required by momentum conservation in the two-body final state, and the sharply decreasing probability of finding a single nucleon in the

---

\* Supported in part by a grant from Research Corporation.

<sup>†</sup> College of William and Mary, Williamsburg, Virginia.

<sup>‡</sup> Physics Institute, University of Neuchatel, Switzerland.

<sup>\*\*</sup> Nuclear Research Center, University of Alberta, Edmonton, Alberta, Canada.

<sup>†\*</sup> Miami University, Oxford, Ohio.

nucleus with the required momentum. The momentum transfer required in a single-nucleon process is  $(A + 1)/(A - 1)$  times greater than the momentum required in a two-nucleon process. ( $A$  is the atomic number of the target nucleus.) Using this assumption Ingram et al<sup>1</sup> have made a calculation based on previous work by Ruderman.<sup>2</sup> This calculation relates the reaction  $A(p, \pi^+)A + 1$  to the elementary reaction  $p(p, \pi^+)d$ . An independent particle model of the nucleus is assumed which allows one to relate the matrix element

$$\langle \pi, A + 1 | T | pA \rangle$$

to the sum of two-nucleon matrix elements of the form

$$\langle \pi d | T' | pp \rangle$$

where  $T$  and  $T'$  are the  $A + 1$  and the two-nucleon operators respectively.

The differential cross section for the reaction  $d(p, \pi^+)t$  resulting from the calculation has the form

$$\left( \frac{d\sigma}{d\Omega} \right)_{pd \rightarrow \pi^+ t}^{CM} = K |F_d(\Delta)|^2 \left( \frac{d\sigma}{d\Omega} \right)_{pp \rightarrow d\pi}^{CM} \quad (1)$$

$K$  is a kinematical factor,  $F_d(\Delta)$  is a form factor and  $d\sigma/d\Omega)pp \rightarrow d\pi$  is the differential cross section for the reaction  $p(p, \pi^+)d$ . All these quantities are evaluated in the center of mass.  $F_d(\Delta)$  can be written as

$$F_d(\Delta) = \int \frac{\Phi_t^*(0, \vec{x})}{\Phi_d(0)} e^{i\Delta \cdot \vec{x}} \Phi_d(\vec{x}) d^3x$$

The Fermi momentum of the proton within the target nucleus,  $\vec{\Delta}$ , is required by kinematics to have the value

$$\vec{\Delta} = \frac{1}{2} \vec{k}_p - \frac{1}{3} \vec{k}_\pi$$

Here  $\vec{k}_p$  and  $\vec{k}_\pi$  are the momenta of the incident proton and created pion respectively in the CM system.  $\Phi_t$  and  $\Phi_d$  are the single-nucleon wave functions of the triton and deuteron.  $\Phi_d(0)$  is required for normalization purposes.  $\vec{x}$  is the relative position of the proton within the deuteron and can be expressed as

$$\vec{x} = \frac{1}{2} (\vec{r}_0 - \vec{r}) - \vec{R}_d$$

where  $\vec{r}_0$ ,  $\vec{r}$ , and  $\vec{R}_d$  are respectively the positions of the incident proton, the target proton, and the center of mass of the deuteron.

The measurement of the differential cross section expressed in equation (1) provides two pieces of information. Primarily it will determine the validity of the two-nucleon approximation. If this approximation is born out by the general shape of the cross section, then specific wave function information can be extracted. The high Fermi momenta involved (360 MeV/c and 465 MeV/c in the backward direction at 470 and 590 MeV) correspond to intra-nucleon distances of less than 1 fm. With information of the deuteron wave function from other experiments,<sup>3</sup> the results from this experiment can provide information about the triton wave function at small distances.

The difficulty in carrying out this measurement is due to the small size of the cross section of the  $d(p, \pi^+)t$  reaction compared to the cross section of other reactions which can occur. These background reactions have cross sections between two and three orders of magnitude larger than the one desired. Some of those occurring from the deuterium target nuclei are  $d(p, p)d$ ,  $d(p, 2p)n$ ,  $d(p, \pi)pNN$ , and  $d(p, \pi\pi)NNN$ . Similar reactions can occur from the carbon in the  $CD_2$  target used in the present experiment.

### Description of the Experimental Setup

The detection system is illustrated in figure 1. It consisted of two charged particle telescopes. The pion arm, which was rotated from  $15^{\circ}$  to  $150^{\circ}$  consisted of three scintillation counters ( $\pi_1$ ,  $\pi_2$ ,  $\pi_3$ ) and three wire spark chambers. The spark chambers consisted of three horizontal and two vertical planes, and were used only to check the distribution of trajectories within the solid angle. Copper absorbers were placed between  $\pi_2$  and  $\pi_3$  to decrease the number of protons and other heavy particles from the background. A coincidence ( $\pi_1 \cdot \pi_2 \cdot \pi_3$ ) was required to define a particle in this arm. The dynode signal from  $\pi_2$  was also used to measure the  $dE/dx$  of this particle;  $\pi_2$  defined the solid angle of the reaction for all angles studied. For large (backward) angles,  $\pi_2$  was 17.8 cm wide, 12.7 cm high and 0.635 cm thick and was located 127.5 cm from the target. For the smaller (forward) angles  $\pi_2$  was either  $12.8 \times 7.6 \times 0.635 \text{ cm}^3$  or  $10.2 \times 7.6 \times 0.635 \text{ cm}^3$ . Its distance from the target varied with angle.  $\pi_1$  was  $12.8 \times 10.2 \times 0.159 \text{ cm}^3$  and remained a distance of 47.8 cm from the target throughout the experiment.  $\pi_3$  was  $22.9 \times 17.8 \times 0.635 \text{ cm}^3$  and normally was located 14.5 cm behind  $\pi_2$ .

The triton arm which was rotated from  $4.2^{\circ}$  to  $15.5^{\circ}$  consisted of four scintillation counters ( $T_1$ ,  $T_2$ ,  $T_3$ ,  $T_4$ ). Absorbers of aluminum and copper were placed between  $T_3$  and  $T_4$ . The thickness of these absorbers was always large enough to stop all tritons. Thus, a particle in this arm was defined by the coincidence ( $T_1 \cdot T_2 \cdot T_3 \cdot \bar{T}_4$ ). The effect of the anti-coincidence requirement was to reduce the background by about 50% without affecting the number of triton events. An event was defined by the coincidence ( $\pi_1 \cdot \pi_2 \cdot \pi_3 \cdot (T_1 \cdot T_2 \cdot T_3 \cdot \bar{T}_4)$ ). The time-of-flight (TOF) of the particle on the triton arm was measured between  $T_2$  and  $T_3$ . The dynode signal from  $T_3$  was also used to measure the  $dE/dx$  of this particle. The dimensions of  $T_3$  were 30.5 cm wide by 35.5 cm high by 1.26 cm thick. Its distance from the target varied from 406 cm to 559 cm as the angle

varied.  $T_4$  had the same dimensions as  $T_3$  and was mounted two inches behind it. The solid angle was defined on the triton arm by  $T_3$ . In general, this solid angle was overdetermined by a factor of two with respect to the defining solid angle on the pion side. In this way, the affects of multiple Coulomb scattering were kept negligible.

As a measure of the number of chance coincident events within a given telescope, the signal from one of the counters was delayed 56ns (the time between beam bursts); and the number of coincidences between this signal and the other counters in the telescope was recorded. This was done for the pion and triton arms, the event signal and the monitor telescope.

When a coincidence was observed between the pion and the triton arms, the TOF and  $dE/dx$  from the triton arm along with the  $dE/dx$  and spark chamber data from the pion arm were tagged and entered on magnetic tape through the use of an on-line computer. The TOF and the two  $dE/dx$  were interfaced by three analogue-to-digital converters. The spark chamber data was interfaced by a commercial digitizing system. The duration of a run along with the total number of monitor counts and events were also recorded on the tape. An on-line analysis of the experiment was carried out.

A  $CD_2$  target of dimensions  $10 \times 10 \times 0.203 \text{ cm}^3$  was used throughout the experiment. It was oriented to minimize multiple scattering on the pion side. A graphite target 0.064 cm thick was used to measure the background contribution due to the carbon in the  $CD_2$  target. It had 66% of the number of carbon nuclei in the  $CD_2$  target.

The experiment was done with proton beams of 470 and 590 MeV at the NASA Space Radiation Effects Laboratory. The 470 MeV beam was produced from the normal 590 MeV beam through the use of a copper degrader. The beam spot for the 590 MeV beam at the target was 3.17 cm in diameter. It had a divergence of less than  $\pm 0.4^\circ$ . The divergence of the 470 MeV beam was the same, and its beam spot at the target was 5.1 cm wide  $\times$  7.6 cm high.

The incident proton intensity was monitored by scattering protons into a three-counter telescope from an auxilliary aluminum target  $30 \times 30 \text{ cm}^2 \times 0.6 \text{ cm}$  thick placed 6 meters downstream from the  $\text{CD}_2$  target. Pictures taken at the monitor target indicated that the beam did not exceed the dimensions of the target region viewed by the monitor telescope. The beam monitor was calibrated using the  $^{12}\text{C}(\text{p}, \text{pn})^{11}\text{C}$  reaction<sup>4</sup> on graphite targets. The number of activated nuclei was determined by counting the annihilation photons of the positrons emitted in the decay of  $^{11}\text{C}$  in a calibrated geometry. A monitor calibration was made each time the energy was changed.

To insure the system was working properly the pp and pd elastic cross sections at one angle were measured before data on the  $d(p, \pi^+)t$  reaction were taken. These measurements agreed with previous measurements within the uncertainty limits.

### Analysis of the Data

The on-line analysis of the spark chamber data provided a knowledge of the distribution of event trajectories in the solid angle defining pion arm. This information was used as a check on the system, but was not directly used in the calculation of the results.

The on-line analysis of the time-of-flight and  $dE/dx$  from the triton arm and the  $dE/dx$  from the pion arm consisted of displaying these spectra in one-dimensional arrays of 50 channels each. To enhance the triton and pion peaks, cuts were placed on each spectrum in the region of the desired peak. Three new spectra were then constructed, each showing the distribution of events which were found within the cuts on the other two spectra. Spectra with the same cuts were taken with the carbon target. These were corrected for monitor counts and number of carbon nuclei so they would correspond to the  $\text{CD}_2$  data. The carbon spectra were then subtracted from the  $\text{CD}_2$  spectra. Any residual background could be extrapolated from the wings of the peaks and subtracted. A satisfactory set of cuts was found when

the number of events in each spectra was the same. These events were assumed to be  $d(p, \pi^+)t$  events. As a check, it was found that if the cuts on one of the spectra were shifted, the peaks in the other two spectra disappeared.

In the TOF and  $dE/dx$  spectra from the triton arm several reactions could be identified. The position of the  $d(p, \pi^+)t$  reaction peak was known from the calibration of the system using the  $pd$  elastic reaction. This peak was generally clearly separated (see fig. 2(a) and (b)) from the more intense and broader peak of the quasi-elastic deuterons. These deuterons are due principally to the reaction  $d(p, \pi^+)dn$ . Proton and deuterons from elastic scattering reactions were almost completely suppressed.

The corresponding peaks in the  $dE/dx$  spectrum from the pion arm were not separated. This was due in part to the resolution of the system. The pions from the  $d(p, \pi^+)t$ , and the  $d(p, \pi^+)np$  reactions occur in the main peak (see fig. 2(c)). However, there was a long tail for large  $dE/dx$  which was, in part, attributed to the muons from pion decays. Thus narrow cuts were not possible on this spectrum.

There were three sources of background due to the carbon in the  $CD_2$  target was subtracted as described above. There remained a background due to the tail of the three-body final state reactions, and a background due to random events (chance coincidences). The contribution of the last two sources was estimated from the shape of the triton peak and the asymptotic values of the spectrum after the carbon background had been subtracted.

After the experiment was completed, an extensive off-line analysis was made. It was found that the number of true events was strongly affected by the cuts which were chosen for the three spectra. To minimize this problem, cuts wide enough to insure that no true events would be eliminated were placed on the  $dE/dx$  spectrum from the pion side. A two-dimensional spectrum of the remaining correlated TOF and  $dE/dx$  events from the triton side was formed (see fig. 3). The triton events appeared localized in an identifiable region.

In order to facilitate the extraction of the true events in this region from the background, it was helpful to smooth both the spectrum from the  $CD_2$  target and the spectrum from the carbon target. This was especially useful for the carbon target, since this spectrum was multiplied by a factor which was usually greater than two and sometimes as large as four. The statistical variation of counts in each channel made the spectrum difficult to analyze unless the smoothing was carried out. The smoothing process consisted of taking a weighted average of the channels surrounding a given channel. This procedure did broaden the event peaks, but it did not change the number of events, so the cross section was not affected.

After carbon subtraction there generally remained a residual background. We interpret this residual background as being due to different numbers of chance coincident events in the  $CD_2$ - and C-runs, and from other reactions on D. The separation of the true events from this residual background was carried out in two different ways. The shape and the width of the TOF spectrum had been determined during pd and pp elastic calibration runs to be gaussian. Using this shape, the three parameters of a gaussian could be determined from the data. The width was required to vary smoothly as a function of angle. When this gaussian was subtracted from the data points, a background resulted which varied in a smooth way under the peak and matched the background on either side. The same procedure was followed for the  $dE/dx$  peak of the triton. A final condition placed on these two fits required they yield the same number of events, within statistics, and a consistent background.

The second method of analysis consisted of assuming a smoothly varying background from outside the peak region to under the peak region. The background in the two-dimensional spectrum was extrapolated in three different directions. From these three backgrounds, which were generally consistent with statistics, a composite background was determined. This composite background was then used to determine the number of true events.

When the two methods of analysis were applied to the same two-dimensional spectrum the results were consistent within statistics.

### Calculation of the Cross Section

The expression used to calculate the differential cross section is

$$\frac{d\sigma}{d\Omega} = \frac{N \cdot \cos \theta_{tgt}}{\Delta\Omega_{\pi} \cdot M_T \cdot C \cdot n_T \cdot E}$$

$N$  is the number of true events determined as described above.  $\theta_{tgt}$  is the angle of the target relative to a plane perpendicular to the beam.  $\Delta\Omega_{\pi}$  is the solid angle defined by counter  $\pi_2$ . The value for  $\Delta\Omega_{\pi}$  was obtained by dividing the area of this counter by its distance from the target squared. No correction for finite beam spot size was necessary. The true number of monitor counts,  $M_T$ , was found by subtracting the monitor chance counts from the monitor counts. The determination of the constant of proportionality,  $C$ , between the beam intensity and the monitor counts is described above.  $n_T$  is the number of deuterons/cm<sup>2</sup> in the target. The efficiency,  $E$ , of the system depends on a number of factors.

Since an absorber was inserted between  $\pi_2$  and  $\pi_3$  to decrease the background, a number of pions were lost. To determine this pion loss, an experiment was carried out with a pion beam of varying energies and different absorber thicknesses. This correction term varied from 1 (no absorber) to 0.72 (for 211 MeV pions and an absorber of two inches). Another correction is needed to take into account the loss of pions through decay. Although the experimentally determined correction takes into account some of this contribution, geometrical effects must be considered. The correction for decay alone is, at worst, 0.85. However, since the decay muon had high probability to go from  $\pi_2$  to  $\pi_3$  and part of this effect has already been taken into account, this number is closer to one. The efficiency of the detectors is so close to one, that any deviation from one is, for the time being, included in the systematic uncertainty of the experiment.

The uncertainty in the cross section measured in this experiment is separated into the usual statistical and systematic categories. The statistical uncertainty arises from the number of events under the triton peak in the  $CD_2$ - and C-spectra. This is indicated in the error bars shown on the data points in figures 4 and 5. The systematic uncertainty is divided into two parts for convenience. The first part is the error in the residual background and the second part contains all other sources of error. The error in the residual background is difficult to estimate. If the difference between the two methods of determining this background is used, 10% is a reasonable number. The error in the second part is due to the uncertainty in solid angle, beam calibration, target angle, and deuterium nuclei in the target. This uncertainty is less than 10%.

### Results and Discussion

The differential cross sections at 470 and 590 MeV are shown in figures 4 and 5, respectively. The dashed curves indicate the predictions of the Ingram calculation with Hulthen and exponential wave functions for the deuteron and triton, respectively. The cross section at 590 MeV seems to agree with the calculation in shape but is systematically higher by about a factor of two. The 470 MeV data does not agree nearly as well. (However, note that the theoretical curve was calculated at 450 MeV.) The shape in the forward direction agrees with the theoretically predicted shape, but the cross section is systematically lower. However, the most striking difference occurs in the backward direction. The theory predicts a slight increase followed by a decrease in the cross section; whereas, the experiment indicates a backward peak. It is interesting to note that at 340 MeV data from Chapman et al<sup>5</sup> and Frank et al<sup>6</sup> indicate a similar cross section with a backward peak. (See fig. 6.)

The 590 MeV result would seem to confirm the predictions of the two nucleon process. Before concluding that the backward peak at 470 MeV is a deficiency of the two-nucleon model, rescattering effects will have to be evaluated. These were not included in the Ingram et al<sup>1</sup> calculation.

## REFERENCES

1. C. H. Q. Ingram, N. W. Tanner, J. J. Domingo, Nucl. Phys. B31, 331 (1971).
2. M. Ruderman, Phys. Rev. 87, 383 (1952).
3. J. C. Alder, W. Dollhopf, C. Lunke, C. F. Perdrisat, W. K. Roberts, P. Kitching, G. Moss, W. C. Olsen, and J. R. Priest, Phys. Rev. C6, 2010 (1972).
4. J. B. Cumming, J. Hudis, A. M. Poskanzer and S. Kaufman, Phys. Rev. 128, 2392 (1962).
5. K. R. Chapman, J. D. Jafar, G. Martelli, T. J. Macmahon, H. B. Van der Raay, D. H. Reading, R. Rubinstein, K. Ruddick, and D. G. Ryan, Nucl. Phys. 57, 499 (1964).
6. W. J. Frank, K. C. Bandtel, R. Madey, and B. J. Moyer, Phys. Rev. 94, 1716 (1954).

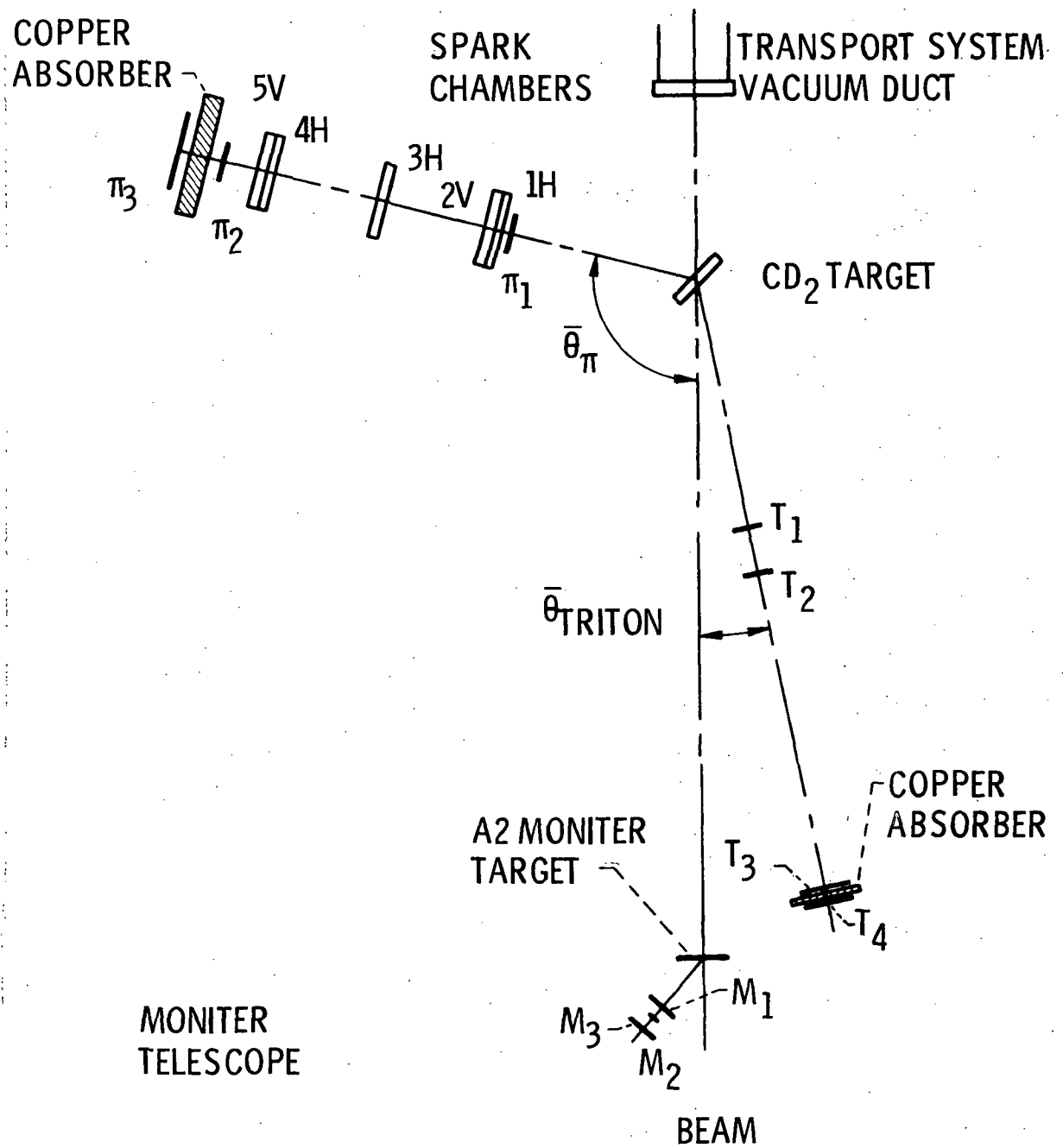


Figure 1. - Experimental setup.

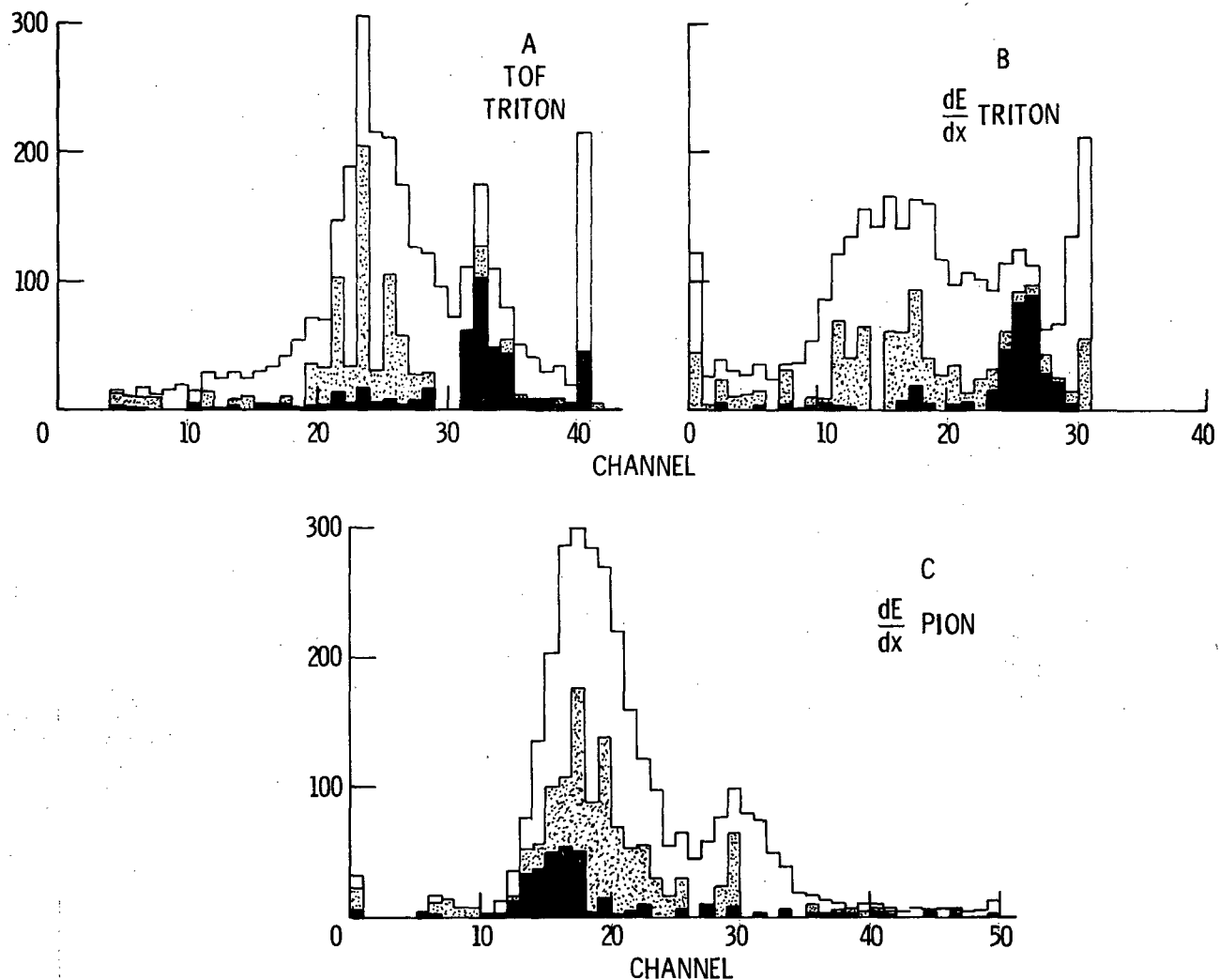


Figure 2. - The one-dimensional spectra taken at 470 MeV with a triton angle of  $10.5^0$  and a pion angle of  $105^0$ . In each of the three cases the total spectrum is the raw spectrum. The stippled area is the spectrum after carbon background subtraction. The shaded region is the spectrum which results when cuts are applied. A is the time of flight (TOF) on the triton side, B is the  $dE/dx$  from the triton side, and C is the  $dE/dx$  from the pion side.

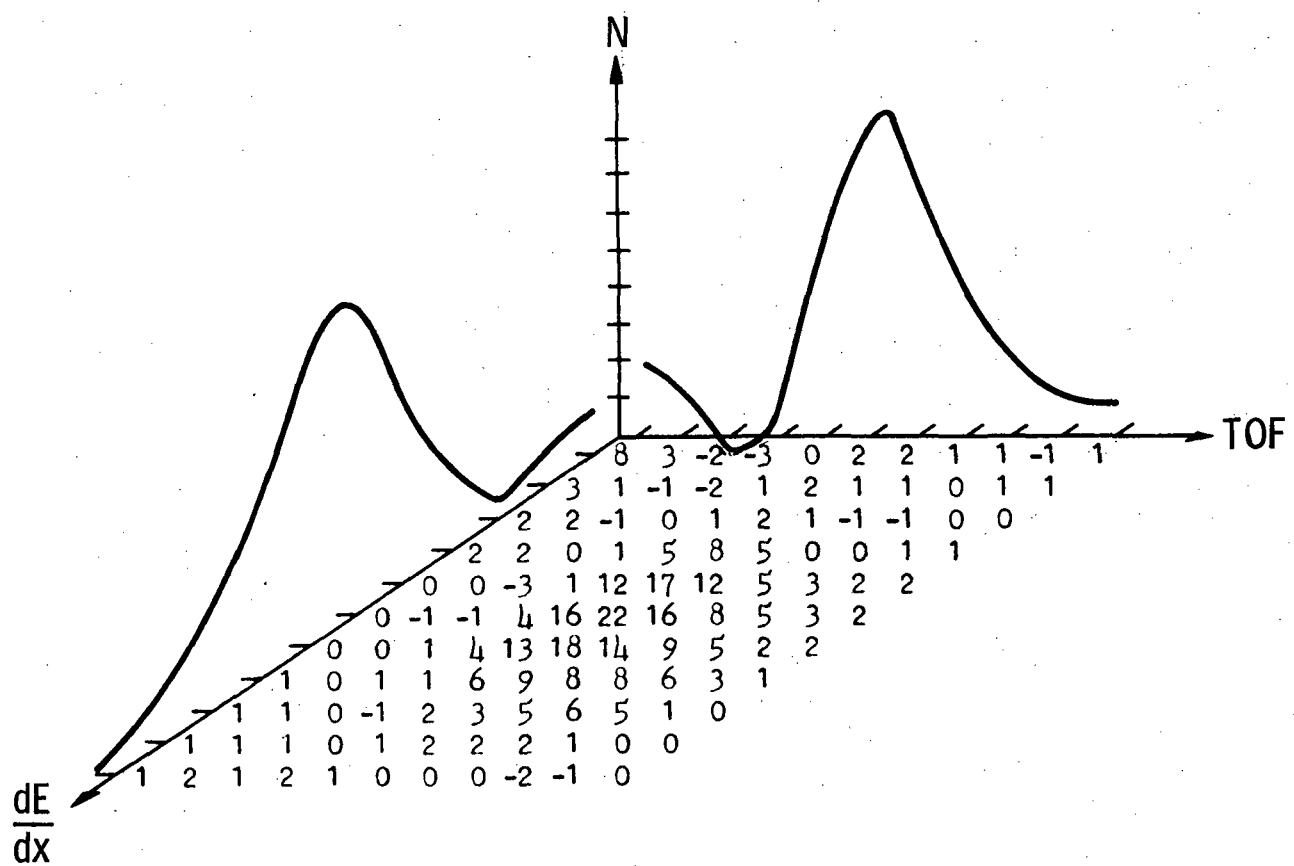


Figure 3. - The two-dimensional spectrum from the correlated time of flight and  $dE/dx$  on the triton side. The background has been subtracted and the spectrum smoothed.

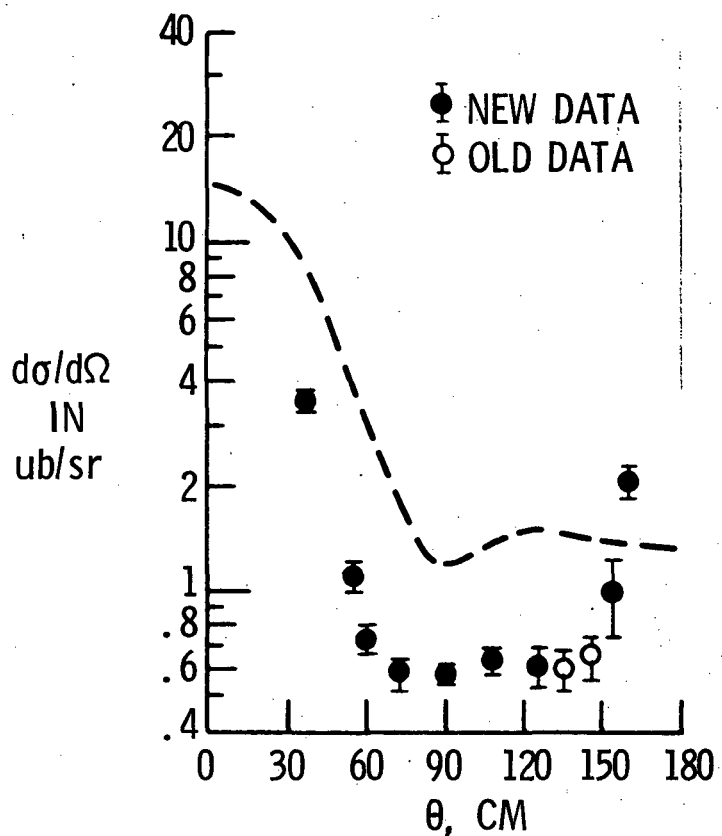


Figure 4. -  $d(p, \pi^+)t$  differential cross section at 470 MeV. The dashed curve is the theoretical prediction using Hulthén and exponential wave functions for the deuteron and triton, respectively.

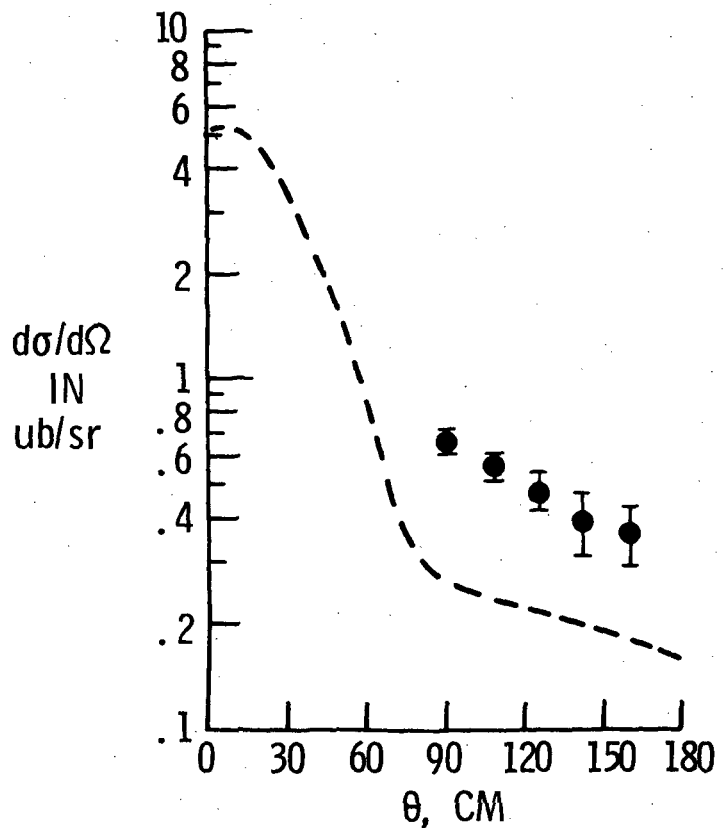


Figure 5. -  $d(p, \pi^+)t$  differential cross section at 590 MeV. The dashed curve is the theoretical prediction using Hulthén and exponential wave functions for the deuteron and triton, respectively.

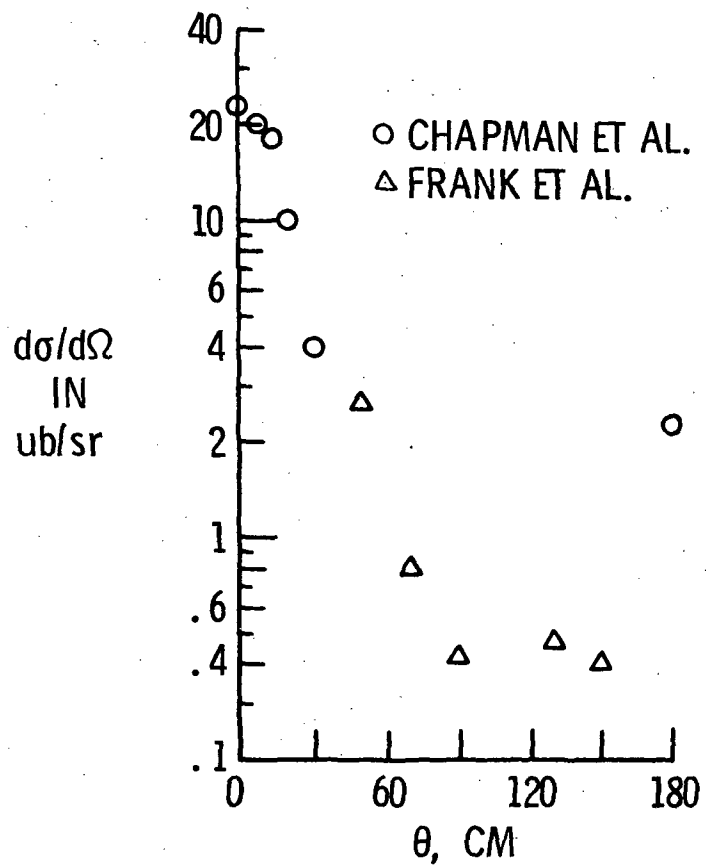


Figure 6. -  $d(p, \pi^+)t$  differential cross section at 340 MeV from data taken by Chapman et al.<sup>5</sup> and Frank et al.<sup>6</sup>.